

## APPENDIX I

In this appendix we shall indicate a technique for numerical integration of (36) and (37). Since the graph of the function to be integrated is merely a cosine wave in  $n\omega_1 t$ , modulated by a uniformly varying function, it is only necessary for the most part to determine the magnitude of the amplitude of the cosine wave from  $\omega_1 t = 0$  to  $\omega_1 t = \pi$ . At  $\omega_1 t = \pi$  an additional correction may have to be made if  $V_{RB}/2V_R$  is not  $\infty$ . The integral of the function will be proportional to the sum of these amplitudes, provided that the distance over which the half cosine waves occur is taken into consideration.

As a simple example, if we consider (12) for  $n = 2$  and  $V_1/V_0 = 1$ , we find we have three peaks occurring approximately at 0,  $\pi/2$  and  $3\pi/8$ . This function is represented in Fig. 12. The respective magnitudes are 2, -1, and 0.19. The integral is then given by

$$b_2 = \frac{4}{\pi} \left[ \frac{\sqrt{2}}{2} - 1.0 + \frac{0.19}{2} \right] = 0.252.$$

The actual value by direct integration is  $b_2 = 0.240$ ; we see the accuracy is fairly good.

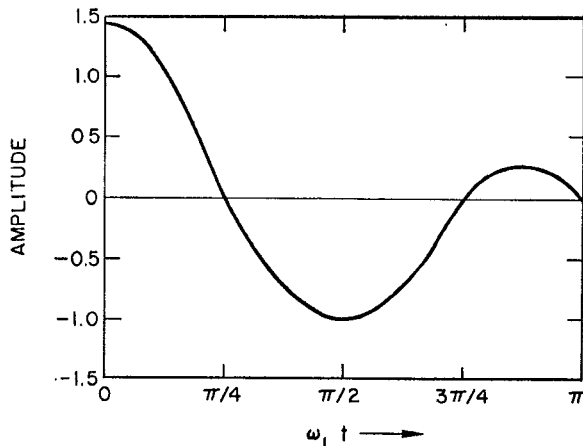


Fig. 12—Variation of second harmonic charge for computation of normalized Fourier coefficient  $b_n$ .

## ACKNOWLEDGMENT

The author is indebted to C. E. Nelson and M. T. Weiss of the Microwave Laboratory, to B. J. Leon and D. R. Anderson of the Research Laboratories, Hughes Aircraft Co., Culver City Calif., for their helpful comments and suggestions.

## A Waveguide Switch Employing the Offset Ring-Switch Junction\*

R. C. JOHNSON†, A. L. HOLLIMAN† AND J. S. HOLLIS‡, MEMBER, IRE

**Summary**—This paper describes an X-band microwave ring switch employing a junction of new design. The insertion loss is less than  $\frac{1}{4}$  db over the design band of 9.0-9.6 kmc; this low loss was obtained through the use of a coupling junction which is designated the offset ring-switch junction. A physical description, the electrical characteristics of the switch, and a qualitative theoretical discussion of the junction are included.

## INTRODUCTION

**R**APID scanning of a sector at a constant rate with a narrow beam antenna, by movement of the complete antenna or by motion of a feed mechanism, imposes the problem of minimizing the

dead-time between scans. Many scanning antennas employ multiple feeds or dishes which rotate at constant speed to limit the dead-time to a reasonable value without forcing the antenna or scanning mechanism to undergo rapid acceleration between scans. Several types of microwave switches have been employed for sequentially switching the input waveguide of such antennas to each of the several feeds or dishes. Waveguide ring switches are often employed for this purpose.

Peeler and Gabriel reported a waveguide ring switch<sup>1</sup> which is based on an annular rotary joint patented by Breetz.<sup>2</sup> This switch employs right-angle bends made of interleaving pins which project into the ring waveguide parallel to the  $E$  field, and couple energy into, and out of, the ring guide. This coupling junction requires the

\* Received by the PGMTT, May 12, 1960; revised manuscript received, June 20, 1960. The work on the switch was supported by the Diamond Ordnance Fuze Laboratories, Washington, D. C., under Contract No. DA-49-186-502-ORD-709; the development of the junction was supported by the U. S. Army Signal Engineering Laboratory, Fort Monmouth, N. J., under Contracts Nos. DA 36-039 SC-72789 and DA 36-039 SC-74870.

† Engineering Experiment Station, Georgia Inst. Tech., Atlanta, Atlanta, Ga.

‡ Scientific-Atlanta, Inc., Atlanta, Ga.

<sup>1</sup> G. D. M. Peeler and W. F. Gabriel, "A volumetric scanning GCA antenna," 1955 IRE NATIONAL CONVENTION RECORD, pt. I, pp. 20-27.

<sup>2</sup> L. D. Breetz, U. S. Patent No. 2,595,186, April 29, 1952. Also, L. D. Breetz, "A Waveguide Rotary Joint with Waveguide Feed," Naval Res. Lab., Washington, D. C., NRL Rept. 3795; January 18, 1951.

ring waveguide to be split longitudinally along two corners. Since the current density across the corners is large, efficient chokes are required along the gaps to prevent excessive loss; these chokes are serrated to prevent longitudinal propagation of energy in the choke grooves.

Tomiyasu reported a waveguide rotary joint<sup>3</sup> which can be adapted for a ring switch. This joint is based upon the use of cascaded Transvar couplers which couple energy into, or out of, the ring waveguide; since the ring waveguide is split longitudinally along high cross-current lines, serrated chokes are employed as in the Breetz rotary joint.

In the design of a waveguide ring switch, it is desirable to make the longitudinal split in the ring guide at the center of the *H*-plane wall, since the only currents that exist across the gap with this configuration are located in the immediate vicinity of the junction. Configurations of this type were proposed independently by Hollis and Long<sup>4</sup> at Georgia Tech, Atlanta, and by Coleman<sup>5</sup> at the U. S. Navy Electronics Laboratory. A *K<sub>u</sub>*-band switch based upon this principle was fabricated at Georgia Tech.<sup>6</sup> This switch operated satisfactorily; however, the bandwidth was limited to about 2 per cent by the impedance characteristics of the input and output junctions. An alternate coupling configuration has been developed at Georgia Tech, which has inherent broad bandwidth characteristics, and which can be scaled for use at any frequency in the microwave region; this coupling junction is called the *offset ring-switch junction*.<sup>7</sup> The switch described in this paper employs junctions of this type.

#### OFFSET RING-SWITCH JUNCTION

The offset junction consists of a cavity, of length *a* and width *b*, which is used as a coupling device between two rectangular waveguides as illustrated by the section, through a typical junction, in Fig. 1. The lines down the center of the upper waveguide represent a mechanical separation which permits relative motion between sections *A* and *B*.

The junction has a simple geometrical configuration which requires no additional matching devices. Its performance is independent of the *E* dimension, since all discontinuities are parallel to the *E* field. In the junction cavity, the width *b*, which is approximately one and a half times the width of the coupled guides, is

large enough to propagate both the  $TE_{10}$  and  $TE_{20}$  modes; the impedance characteristics of the junction result from interaction of the energy in these modes. A rigorous theoretical analysis of the junction has not been completed; however, the following semiquantitative analysis serves to indicate the principle of operation.

The offset junction is a bilateral device; however, in this discussion it will be assumed that the energy is coupled from guide 1 into guide 2. At the discontinuity between guide 1 and the cavity, all  $TE_{m0}$  modes are excited; but only the  $TE_{10}$  and  $TE_{20}$  modes are above cutoff frequency. Consider the behavior of these two modes. The  $TE_{10}$  mode energy has a lower phase velocity than the  $TE_{20}$  mode energy; therefore, their relative phase changes as they propagate down the cavity. If the total relative phase shift in the cavity is  $\pi$ , all the energy is coupled from guide 1 into guide 2. This situation is illustrated in Fig. 2; notice that the boundary conditions at the ends of the cavity are roughly satisfied if the phase and amplitude of each mode are as illustrated.

The total relative phase shift in the junction cavity is

$$\theta_r = \theta_{10} - \theta_{20}$$

or

$$\theta_r = 2\pi a_e \left( \frac{1}{\lambda_{g10}} - \frac{1}{\lambda_{g20}} \right), \quad (1)$$

where  $\theta_{10}$  and  $\theta_{20}$  are the phase changes of the  $TE_{10}$  and  $TE_{20}$  modes, respectively;  $a_e$  is the electrical length of the cavity, and  $\lambda_{g10}$  and  $\lambda_{g20}$  are the guide wavelengths in the cavity of the  $TE_{10}$  and  $TE_{20}$  modes, respectively. Because of the cavity end effects, the electrical length of the cavity  $a_e$ , is slightly longer than the physical length *a*.

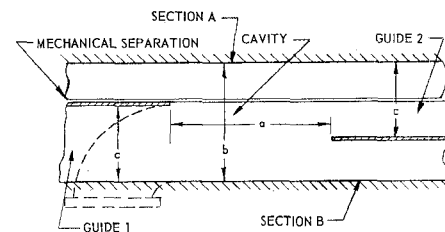


Fig. 1—The basic geometry of the offset junction. The *E* field is perpendicular to the plane of the page; therefore, *c* is the *H* dimension of guide 1 and guide 2. The dashed lines indicate the possible addition of an *H*-plane bend to guide 1 for use in a ring switch.

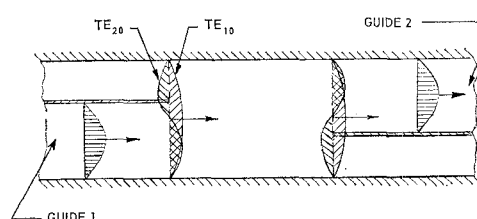


Fig. 2—The propagating modes in the offset junction. The curves represent the *E*-field amplitude, and the arrows represent the direction of propagation.

<sup>3</sup> K. Tomiyasu, "A new annular waveguide rotary joint," Proc. IRE, vol. 44, pp. 548-553; April, 1956.

<sup>4</sup> R. E. Horner, J. S. Hollis, M. W. Long, et al., "Two-Beam 16,000-mc Modified Luneberg Lens Scanning System," Georgia Inst. Tech., Atlanta, Final Rept., Contract No. DA 36-039 SC-15566, p. 13; February 15, 1953. U. S. Patent No. 2,826,742, March 11, 1958.

<sup>5</sup> G. M. Coleman, U. S. Navy Electronics Lab., San Diego, Calif., unpublished memoranda.

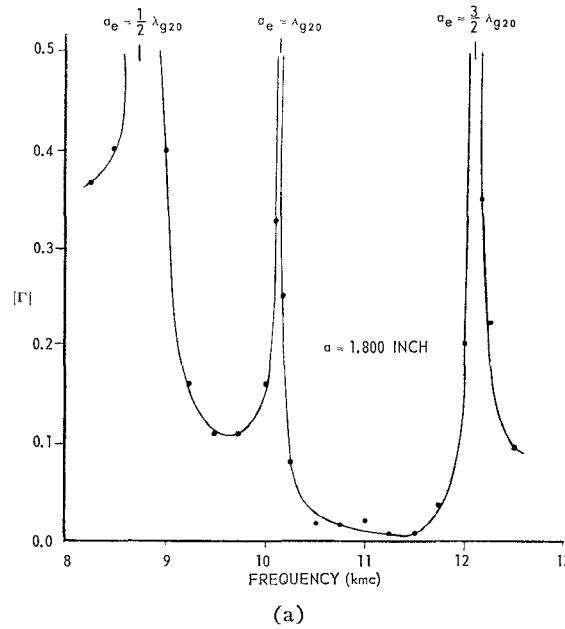
<sup>6</sup> R. D. Hayes and J. S. Hollis, "A Modification Kit for the Two-Beam 16,000-mc Modified Luneberg Lens Scanning System," Georgia Inst. Tech., Atlanta, Final Rept., vol. III, Contract No. DA 36-039 SC-42707; September 15, 1955.

<sup>7</sup> J. S. Hollis, patent pending.

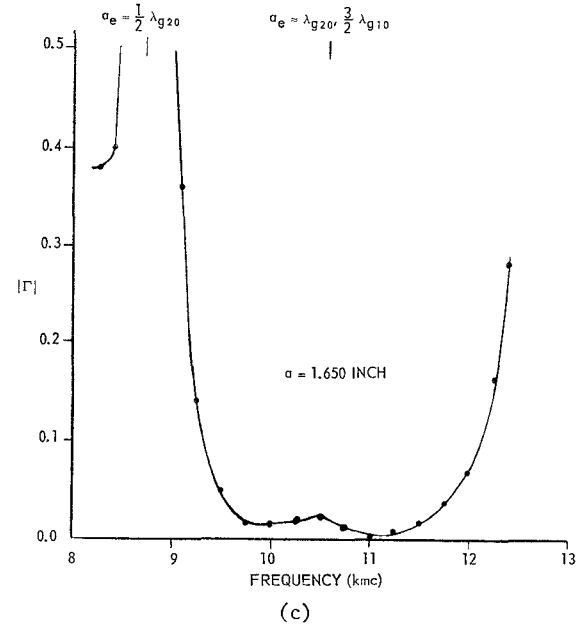
The magnitude of the reflection coefficient has been measured for offset junctions having various cavity lengths  $a$ , with  $b = 1.400$  inches and  $c = 0.900$  inch. The  $E$  dimension was 0.400 inch throughout, and the interior walls had a thickness of 0.040 inch. In offset junctions with these dimensions, the electrical length of the cavity appeared to be about  $13\frac{1}{2}$  per cent of a free-space wavelength longer than the physical length. A curve of the magnitude of the reflection coefficient,  $|\Gamma|$ , vs frequency for a typical junction is shown in Fig. 3(a). The total relative phase shift in this cavity was calculated to be  $\pi$  for a frequency of 11.12 kmc; note that the

junction operates well in a region near this frequency. The three resonances in the band occur at frequencies such that the electrical length of the cavity is an integral number of half-wavelengths for the  $TE_{20}$  mode. This same type of impedance vs frequency characteristic with regularly spaced  $TE_{20}$  mode resonances has been observed for many junctions of various cavity lengths.

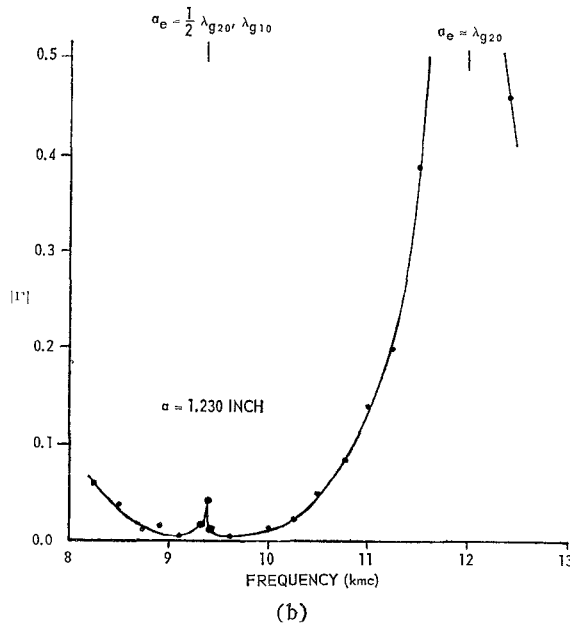
In practice, it has been found that the  $TE_{20}$  mode resonance is greatly reduced, or not present, if the electrical length of the cavity is simultaneously  $n$  half-wavelengths long for the  $TE_{20}$  mode and  $n+1$  half-wavelengths long for the  $TE_{10}$  mode, where  $n$  is a posi-



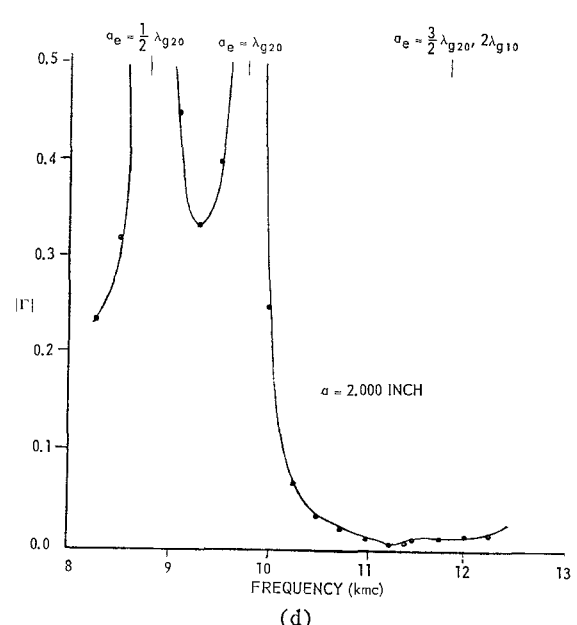
(a)



(c)



(b)



(d)

Fig. 3—The magnitude of the reflection coefficient,  $|\Gamma|$ , vs frequency for junctions having cavity widths  $b = 1.400$  inches and cavity lengths  $a$  as indicated;  $a_e$  = electrical length of cavity.

tive integer. This condition can be expressed mathematically as two simultaneous equations,

$$a_e = \frac{n\lambda_{g20}}{2} = \frac{n\lambda}{2\sqrt{1 - (\lambda/b)^2}} \quad (2)$$

$$a_e = \frac{(n+1)\lambda_{g10}}{2} = \frac{(n+1)\lambda}{2\sqrt{1 - (\lambda/2b)^2}} \quad (3)$$

where  $\lambda$  is the free space wavelength. Solving these equations, it is found that the electrical length and the width of the cavity must be the following:

$$a_e = \lambda \left[ \frac{3n^2 + 8n + 4}{12} \right]^{1/2} \quad (4)$$

$$b = \lambda \left[ \frac{3n^2 + 8n + 4}{8n + 4} \right]^{1/2}. \quad (5)$$

If  $b$  is equal to 1.400 inches, (4) and (5) give the values of  $a_e$  in Table I. The frequency,  $f_0$ , corresponds to a free space wavelength of  $\lambda$ , and the physical length,

TABLE I

$n$	$\lambda$ (inch)	$f_0$ (kmec)	$a_e$ (inch)	$b$ (inch)	$a$ (inch)
1	1.252	9.43	1.400	1.400	1.231
2	1.107	10.66	1.807	1.400	1.658
3	0.999	11.81	2.139	1.400	2.004

$a$ , was estimated by subtracting  $0.135\lambda$  from the electrical length,  $a_e$ . The magnitude of the reflection coefficient was measured over a wide band of frequencies for three junctions having dimensions close to those given in Table I. The  $TE_{20}$  mode resonance was not observed for the cases  $n=2$  and 3, as shown in Figs. 3(c) and 3(d), respectively, and it was greatly reduced for the case  $n=1$ , as shown in Fig. 3(b). It is possible that the latter resonance can be eliminated by a slight change in the dimension  $a$ . Experimental evidence indicated that the resonances for junctions corresponding to cases 1, 2, and 3 tend to occur at frequencies which are 0.3, 0.8 and 2.5 per cent, respectively, lower than theoretically predicted in Table I.

The three cavities of Table I produced wide bandwidth junctions which can be scaled to other frequencies. The power handling capacity is limited at the resonant frequency  $f_0$ ; but there is a relatively wide band of frequencies on each side of  $f_0$  where the junction will transmit high power. In low-power devices, such as radiometers, this power limitation at  $f_0$  is not a disadvantage.

A qualitative argument for the wide bandwidth characteristics of the offset junction is illustrated in Fig. 4; the phase shift of each mode and the relative phase shift are shown as functions of frequency for a junction corresponding to  $n=2$  in Table I. It should be noted that the relative phase shift is more nearly constant than the phase shift of either mode. The electrical

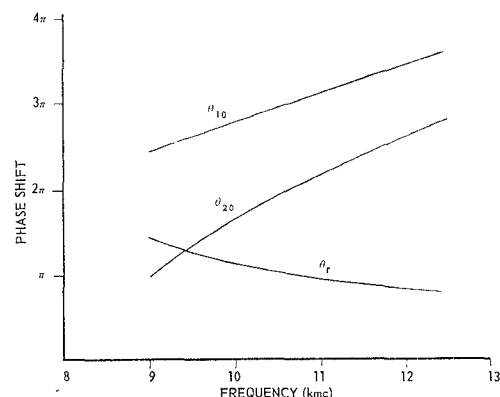


Fig. 4—The total phase shift for the  $TE_{10}$  and  $TE_{20}$  modes and their relative phase shift in a junction cavity having dimensions  $a_e=1.807$  inches and  $b=1.400$  inches.

length of the cavity was assumed to be constant and identical for both modes; however, in a more detailed analysis,  $a_e$  is a function of frequency and of the mode of propagation.

#### CURVED JUNCTION

Fig. 1 illustrates the manner in which the offset ring-switch junction can be split for use in a ring switch. In this case, guide 2 represents the ring guide which is split down the center of the  $H$  dimension. Since the currents in the guide walls are parallel to the split, except in the junction cavity, chokes are required only in this region, and the loss in the split ring guide is almost as small as that in ordinary waveguide.

The offset junctions described in the previous section were constructed from straight sections of rectangular waveguide; however, the junction performance is not greatly affected if the cavity is curved in the  $E$  plane, as long as the mean cavity length is not changed. To meet physical limitations, the ring guide for the switch which is described below was curved in the  $E$  plane with a mean radius of 4.5 inches (approximately 3.5 wavelengths); the  $E$  dimension was made 0.600 inch to increase power transmission capability and to reduce loss.

The junction cavity selected for this switch had a mean length and width approximately proportional to those used for Fig. 3(b); however, to prevent the occurrence of the resonant peak in the design band of the switch, the cavity dimensions were scaled downward to put the resonance at the high end of the band. This required the  $H$  dimension of the ring guide to be 0.880 inch rather than 0.900 inch of standard RG-52/U waveguide. The magnitude of the reflection coefficient vs frequency for a typical curved junction with this configuration has the same general shape as that for a straight junction.

#### PHYSICAL DESCRIPTION OF SWITCH

The ring switch is shown in Fig. 5 (assembled) and in Fig. 6 (disassembled). The sub-assemblies shown in Fig. 6 were machined from yellow brass, softsoldered

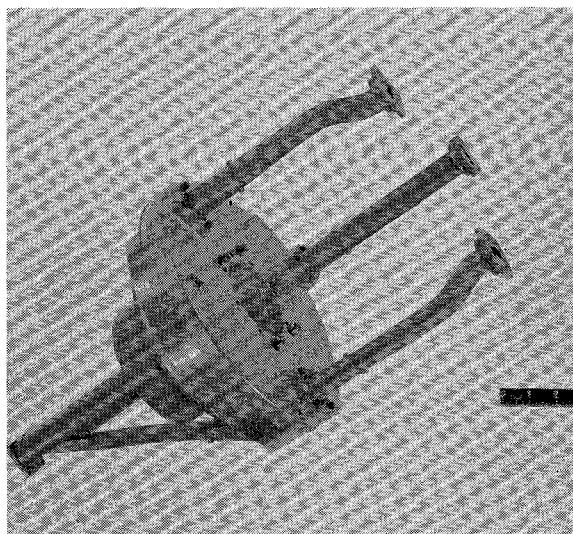


Fig. 5—The ring switch and connecting waveguide assemblies.

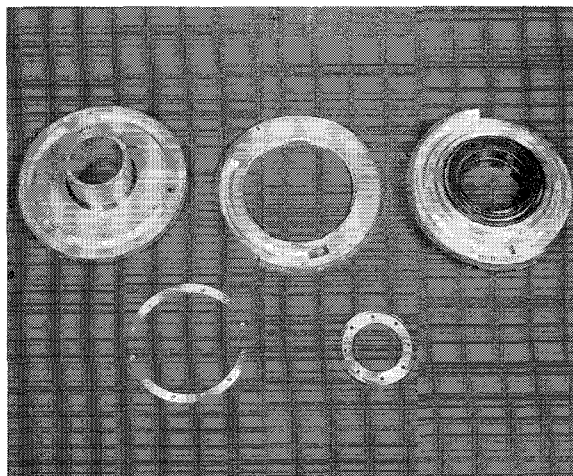


Fig. 6—The ring switch (disassembled).

together, and silver plated. In Fig. 5, the three output arms can be seen on the top surface of the switch, and the input arm is visible at the bottom. The general configuration of the switch and arms was required for compatibility with existing Diamond Ordnance Fuze Laboratories equipment.

Fig. 7 (opposite) is an isometric section of the ring switch, shown with four output arms rather than three, to show the junctions more clearly. The switch is constructed of three principal parts: Part A, the lower section, is stationary, and its input junction is connected to a transmitter-receiver system (see Fig. 5); Part B, the center section, can be manually rotated through  $150^\circ$  to adjust the center of the  $75^\circ$  active sector; Part C, the upper section, rotates at 40 rpm. As the switch rotates, the energy is sequentially switched from one output junction to the next. Fig. 8 (opposite) is an orthographic section through the energy path of the

switch; the dashed line represents the path followed by microwave energy as it propagates through junctions A, B, and C of the switch.

The mean radius of the bend D, and the length of the taper E, in Fig. 7, connecting each of the switch junctions to the external waveguide, were designed to have minimum practical VSWR.

Serrated chokes were used to reduce radiation loss through the gaps between the center section of the switch and the upper and lower sections (see Fig. 6). Those chokes are required only in the vicinity of the junctions, as previously mentioned.

#### SWITCH PERFORMANCE

This ring switch has three output arms spaced  $120^\circ$  apart, and activated sequentially through an active sector of  $75^\circ$ , with the position of the sector adjustable throughout a range of  $150^\circ$ . After the switch had been constructed, electrical measurements were made to determine the following three characteristics of the switch: voltage standing wave ratio, insertion loss, and power transmission capability.

The maximum VSWR was measured for representative frequencies over the operating band and is shown in Fig. 9. The energy transmission path (see Figs. 5, 7 and 8) consisted of the input waveguide, the input taper, a  $90^\circ$  H-plane bend, the input junction, the center section junction, one of the three output junctions, a  $90^\circ$  H-plane bend, an output taper, and the output waveguide terminated with a sliding load. The positions of the center ring and output ring were varied to determine the maximum VSWR at each frequency. The higher VSWR with output arm number 1 is believed to be caused by a nonuniformity in its output waveguide assembly, since before the input and output waveguide assemblies were installed, the maximum VSWR of the switch, with input and output  $90^\circ$  bends and tapers but without the combination twist-bend sections, was 1.12. The limited time available for the development of this switch did not permit additional tests and improvement of the waveguide sections.

The loss through the entire ring switch, including the input and output waveguides, was measured by the substitution method and found to be less than  $\frac{1}{4}$  db over the design band for representative switch positions.

The switch transmitted 200 kilowatts of peak power at atmospheric pressure without breakdown. Since this was the largest power source available for test purposes, the breakdown power could not be measured. With 15-psig pressurization, it is estimated that the switch will transmit a peak power greater than 600 kw.

Approximately  $45^\circ$  of switch rotation is required for switching between successive output arms; thus, the maximum usable scan sector is approximately  $75^\circ$ .

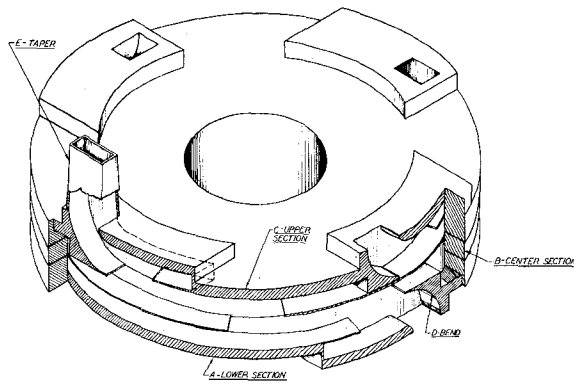


Fig. 7—An isometric section of the *X*-band microwave ring switch shown with four output arms, rather than three, in order to show junctions more clearly.

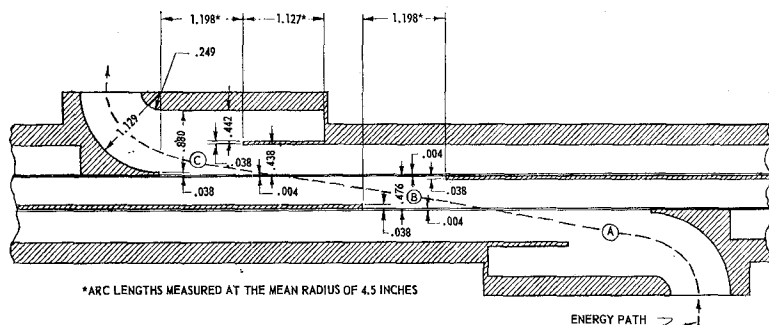


Fig. 8—A section through the energy path of the switch. Junctions *A*, *B*, and *C* are shown.

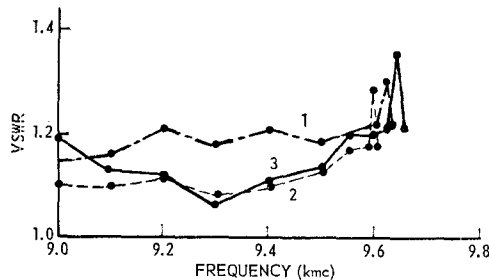


Fig. 9—The maximum VSWR vs frequency for each of the output arms. The energy path includes the total path through the ring switch and external waveguide as shown in Fig. 5.

#### CONCLUSIONS

The waveguide ring switch described in this paper has electrical characteristics which are made possible by the use of the offset ring-switch junction. This junction has a larger switching angle than some other junctions which have been employed in ring switches; however, this fact is more than compensated by the following advantages. 1) The junction has low-loss, wide-bandwidth characteristics. 2) It has a simple geometrical configuration which requires no additional matching devices; this allows the junction to be fabricated with

relative ease for use at millimeter wavelengths. At these wavelengths, the switch diameter is much greater than a wavelength, and the switching angle becomes less significant. 3) The ring-guide is split down the center of the *H* dimension; this eliminates the need for chokes, except in the vicinity of the junction cavity, and it reduces the losses in the split ring-guide. 4) The junction operation is independent of the *E* dimension. In many applications, losses in the ring-guide can be reduced considerably by making the *E* dimension greater than half a wavelength; this is particularly useful at millimeter wavelengths. An increased *E* dimension also reduces the current density orthogonal to the split in the cavity; low-loss junctions have been fabricated without the use of chokes by making the *E* dimension  $1\frac{3}{8}\lambda$ . 5) The offset ring switch junction is capable of handling high power, except at the resonant frequency.

A simplification of the mechanical design and fabrication of this switch could be made by locating the serrated chokes only on the center section of the switch (see Fig. 6); it would then be possible to electroform the upper and lower sections of the switch as integral units. This design change would reduce the required machine work and eliminate almost all of the soldered mechanical joints along the boundaries of the energy path.